Tangent response in coupled dynamical systems

Yan Hua(闫 华)†, Wei Ping(魏 平), and Xiao Xian-Ci(肖先赐)

School of Electronic Engineering, University of Electronic Science and Technology of China, Chengdu 611731, *China*

(Received 3 December 2009; revised manuscript received 24 March 2010)

We construct new unidirectional coupling schemes for autonomous and nonautonomous drive systems, respectively. Each of these schemes makes the state of the response system asymptotically approach the first-order derivative of the state of the driver. From the point of view of geometry, the first-order derivative of the state of the driver can be viewed as a tangent vector of the trajectory of the driver, so the proposed schemes are named tangent response schemes. Numerical simulations of the Lorenz system and the forced Duffing oscillator verify the validity of the tangent response schemes. We further point out that the tangent response can be interpreted as a special kind of generalised synchronisation, thereby explaining why the response system can exhibit rich geometrical structures in its state space.

Keywords: tangent response, generalised synchronisation, coupled dynamical systems

PACC: 0545

1. Introduction

Two or more dynamical systems can realise coupling through the transmission of signals and the systems with appropriate coupling can exhibit interesting dynamical behaviours, such as the synchronisation of chaotic systems. The evolutions of two identical chaotic systems with exactly the same initial conditions will remain the same all the time. But slight differences in initial conditions between them make the trajectories of the two systems diverge exponentially from each other and become uncorrelated in a short time, which is called the property of sensitive dependence on initial conditions. This property shows that the synchronisation between two chaotic systems can be easily destroyed by slight perturbations. This makes it difficult for chaotic systems to synchronise with each other. Therefore, chaotic synchronisation aims to design an appropriate coupling between two systems so that their evolutions can satisfy a certain relationship in the asymptotic sense (for example, an identical relationship) though their initial conditions are different.

In 1990, Pecora and Carroll[1] published their seminal paper, which stimulated intense research activities on the synchronisation of chaotic systems. Since then, various chaotic synchronisation schemes have been proposed and they can be subdivided into six major classes: complete synchronisation,[1,2] generalised synchronisation (GS),[3−8] phase synchronisation,[9−12] lag synchronisation,[12−15] anticipating synchronisation,[16−19] and projective synchronisation.[20−22] Besides, a substantial amount of research has also been done on the applications of chaotic synchronisation, especially in the realm of communications.[23−28]

For each of the above-mentioned synchronisation schemes, there is a certain relationship between the states of the drive system and the response system. More specifically, there is an identical relationship for the complete synchronisation and a certain functional relationship for the GS. The phase synchronisation refers to a property of a chaotic flow called a phase, which has various different definitions.[29] When the absolute value of the difference in trajectory phase between two dynamical systems is less than a specified small positive number, the phase synchronisation occurs. This means that for the phase synchronisation, there exists a nearly identical relationship between the phases of the states of the two systems. For the lag or anticipating synchronisation, the trajectory of the response system is a delayed or advanced version of the trajectory of the driver, which implies a coincidence of time-shifted states of the drive system and the response system. The projective synchronisation means that the states of the drive system and the response system synchronise up to a constant ratio. In other words, there is a proportional relationship between the states of the drive system and the response system. In conclusion, in all the above synchronisation schemes, the state of the response system can in some way reflect the state of the driver or a cer-

†Corresponding author. E-mail: yhyhyanhua@gmail.com

© 2010 Chinese Physical Society and IOP Publishing Ltd

tain property of it, say the phase. But in some cases, besides the state of a dynamical system, the instantaneous rate of change of the state may also be very important. Consider the following situations. When the movement of a particle is studied, the instantaneous velocity of the particle indicates how fast and in which direction it moves at that moment. When the change in weather is studied, one is concerned with air temperature as well as its instantaneous rate of change since the latter indicates how fast the temperature changes. Besides the above two examples, it is well known that many physical phenomena can be described by differential equations which may involve the first-order derivatives of some variables with respect to time, i.e., the instantaneous rates of change of these variables. In some instances, the solutions of equations exist but the equations cannot be solved analytically. This implies that for some physical phenomena, it is difficult and sometimes impossible to describe them with exact expressions. However, the description with differential equations may be possible and grasps the essence of the phenomena. From the point of view of geometry, the instantaneous rate of change can be viewed as the tangent vector of the evolving trajectory of the dynamical system. Therefore, the above discussion indicates that the research on tangent vector is not only of theoretical significance but also of physical and practical importance.

In this paper, we propose new coupling schemes named tangent response (TR) schemes for which the coupling mechanism is unidirectional. The state of the response system of the TR scheme is not directly related to the state of the driver but to the tangent vector of the trajectory of the driver, which is different from the above-mentioned existing schemes. More precisely, after some transient time, the state of the response system at time t will be equal to the tangent vector of the trajectory of the driver at time t. In other words, the state of the response system reflects the rate at which the state of the driver changes with time. We also point out that the TR can be interpreted as a special kind of GS and this interpretation indicates that the coordinate system of the state space of the response system is a nonlinear transformation of the one of the driver.

The rest of the present article is organised as follows. In Section 2, the principles of the TR schemes are presented. Then in Section 3, some numerical simulations are performed to verify the validity of the proposed schemes and we interpret the TR as a special kind of GS. Finally, we summarise our results in Section 4.

2. Principles of tangent response schemes

As we have mentioned in Section 1, the coupling mechanism of the TR scheme is unidirectional and in this section, we first consider the case where the drive system satisfies the following autonomous system of first-order ordinary differential equations:

$$\dot{\boldsymbol{x}}(t) = \boldsymbol{G}(\boldsymbol{x}(t)), \tag{1}$$

where $\boldsymbol{x}(t) \in \mathbb{R}^n$ represents the n-dimensional state vector of the driver at time t and $\boldsymbol{G}$ is a map from U to $\mathbb{R}^n$, with U being an open set in $\mathbb{R}^n$.

To construct the TR scheme, we first utilise the linear–nonlinear decomposition method[30,31] to decompose the term $\boldsymbol{G}(\boldsymbol{x}(t))$ as follows:

$$\boldsymbol{G}(\boldsymbol{x}(t)) = \boldsymbol{A}\boldsymbol{x}(t) + \boldsymbol{F}(\boldsymbol{x}(t)). \tag{2}$$

The following conditions should be satisfied for this decomposition: (i) $\boldsymbol{A}$ is an $n \times n$ real constant matrix and the real parts of whose eigenvalues are all negative and (ii) the map $\boldsymbol{F}$ is differentiable in U, which implies that the Jacobian matrix of $\boldsymbol{F}$ exists. Condition (i), which is also mentioned in Refs. [30] and [31], ensures that the synchronisation can be achieved and condition (ii) is necessary for the construction of the response system. Combining Eqs. (1) and (2), drive system (1) becomes

$$\dot{\boldsymbol{x}}(t) = \boldsymbol{A}\boldsymbol{x}(t) + \boldsymbol{F}(\boldsymbol{x}(t)). \tag{3}$$

The response system is

$$\dot{\boldsymbol{y}}(t) = \boldsymbol{A}\boldsymbol{y}(t) + \mathrm{D}\boldsymbol{F}(\boldsymbol{x}(t))(\boldsymbol{A}\boldsymbol{x}(t) + \boldsymbol{F}(\boldsymbol{x}(t))), \tag{4}$$

where $\mathrm{D}\boldsymbol{F}(\boldsymbol{x}(t))$ denotes the Jacobian matrix of $\boldsymbol{F}$ at $\boldsymbol{x}(t)$, i.e., if $\boldsymbol{F}(\boldsymbol{x}) = (F_1(\boldsymbol{x}), \ldots, F_n(\boldsymbol{x}))^{\mathrm{T}}$ (the superscript T denotes transpose) and $\boldsymbol{x} = (x_1, \ldots, x_n)^{\mathrm{T}}$, then $\mathrm{D}\boldsymbol{F}(\boldsymbol{x}(t)) = ((\partial F_k/\partial x_l)(\boldsymbol{x}(t)))_{k,l=1,\ldots,n}$, where k and l are the row index and the column index, respectively.

The state $\boldsymbol{y}(t)$ of response system (4) asymptotically approaches the first-order derivative of the state $\boldsymbol{x}(t)$ of driver (3), i.e., the invariant manifold of systems (3) and (4) is $\boldsymbol{y}(t) = \dot{\boldsymbol{x}}(t)$. This can be proved by showing that the difference between $\boldsymbol{y}(t)$ and $\dot{\boldsymbol{x}}(t)$ tends to the n-dimensional zero vector as t tends to plus infinity. Let $\boldsymbol{\Delta}(t) = \boldsymbol{y}(t) - \dot{\boldsymbol{x}}(t)$, hence $\dot{\boldsymbol{\Delta}}(t) = \dot{\boldsymbol{y}}(t) - \ddot{x}(t)$. According

to Eq. (3), we have $\ddot{\boldsymbol{x}}(t) = \boldsymbol{A}\dot{\boldsymbol{x}}(t) + \mathrm{D}\boldsymbol{F}(\boldsymbol{x}(t))\dot{\boldsymbol{x}}(t) = \boldsymbol{A}\dot{\boldsymbol{x}}(t) + \mathrm{D}\boldsymbol{F}(\boldsymbol{x}(t))(\boldsymbol{A}\boldsymbol{x}(t) + \boldsymbol{F}(\boldsymbol{x}(t)))$. Subtracting it from Eq. (4) yields $\dot{\boldsymbol{y}}(t) - \ddot{\boldsymbol{x}}(t) = \boldsymbol{A}\boldsymbol{y}(t) - \boldsymbol{A}\dot{\boldsymbol{x}}(t)$, which is equivalent to $\dot{\boldsymbol{\Delta}}(t) = \boldsymbol{A}\boldsymbol{\Delta}(t)$. Since all the eigenvalues of $\boldsymbol{A}$ have negative real parts, $\boldsymbol{\Delta}(t)$ converges to the zero vector in the limit $t \to \infty$ as expected.

When the driver is a nonautonomous system of first-order ordinary differential equations, the scheme can be described as follows.

The driver for this case can be expressed as

$$\dot{\boldsymbol{x}}(t) = \boldsymbol{G}(t, \boldsymbol{x}(t)), \tag{5}$$

where $\boldsymbol{G}$ is a map from an open set $U \subset \mathbb{R}^{n+1}$ to $\mathbb{R}^n$. The term on the right-hand side of Eq. (5) is decomposed into two parts

$$\boldsymbol{G}(t, \boldsymbol{x}(t)) = \boldsymbol{A}\boldsymbol{x}(t) + \boldsymbol{F}(t, \boldsymbol{x}(t)). \tag{6}$$

For this decomposition, the matrix $\boldsymbol{A}$ and the map $\boldsymbol{F}$ should satisfy exactly the same conditions as those for $\boldsymbol{A}$ and $\boldsymbol{F}$ in Eq. (2). Then the driver can be written in the following form:

$$\dot{\boldsymbol{x}}(t) = \boldsymbol{A}\boldsymbol{x}(t) + \boldsymbol{F}(t, \boldsymbol{x}(t)). \tag{7}$$

The corresponding response system is

$$\begin{aligned}\dot{\boldsymbol{y}}(t) \;=\; & \boldsymbol{A}\boldsymbol{y}(t) + \boldsymbol{F}_t(t, \boldsymbol{x}(t)) \\ & + \boldsymbol{F}_{\boldsymbol{x}}(t, \boldsymbol{x}(t))(\boldsymbol{A}\boldsymbol{x}(t) + \boldsymbol{F}(t, \boldsymbol{x}(t))),\end{aligned} \tag{8}$$

where $\boldsymbol{F}_t(t, \boldsymbol{x}(t)) = ((\partial F_k/\partial\tau)(\tau, \boldsymbol{x}(t))|_{\tau=t})_{k=1,\ldots,n}$ is an n-dimensional column vector and $\boldsymbol{F}_{\boldsymbol{x}}(t, \boldsymbol{x}(t)) = ((\partial F_k/\partial x_l)(t, \boldsymbol{x}(t)))_{k,l=1,\ldots,n}$ is a square matrix of dimension n.

Following a similar process to the above, one can easily prove that the invariant manifold of systems (7) and (8) is $\boldsymbol{y}(t) = \dot{\boldsymbol{x}}(t)$, which is the same as that in the autonomous case.

In this section, we have described the basic principles of TR. In the next section, some simulation results are presented and the TR is interpreted as a special kind of GS.

3. Numerical simulations of tangent response and its interpretation as generalised synchronisation

To verify the validity of the TR schemes, some numerical simulations are carried out and the results are presented in this section. Rich geometrical structures are found in the state space of the response system, and in order to understand this, we also discuss in this section the interpretation of TR as a special kind of GS.

First, we consider the case where the driver is autonomous. The driver is chosen as the famous Lorenz system:[32]

$$\begin{aligned}\dot{x}_1 &= -\sigma x_1 + \sigma x_2, \\ \dot{x}_2 &= r x_1 - x_2 - x_1 x_3, \\ \dot{x}_3 &= -b x_3 + x_1 x_2,\end{aligned} \tag{9}$$

where $\sigma = 10$, $r = 28$, and $b = 8/3$. Two different decompositions of the terms on the right-hand side of Eq. (9) are considered, which lead to two different ways of convergence of the error vector $\boldsymbol{\Delta}(t)$. For the first way, the matrix $\boldsymbol{A}$ and the corresponding $\boldsymbol{F}(\boldsymbol{x}(t))$ are as follows:

$$\begin{aligned}\boldsymbol{A} &= \begin{bmatrix} -6 & 0 & 0 \\ 0 & -3 & 0 \\ 0 & 0 & -1 \end{bmatrix}, \\ \boldsymbol{F}(\boldsymbol{x}(t)) &= \begin{pmatrix} -\sigma x_1 + \sigma x_2 + 6x_1 \\ r x_1 - x_2 - x_1 x_3 + 3x_2 \\ -b x_3 + x_1 x_2 + x_3 \end{pmatrix},\end{aligned} \tag{10}$$

which obviously satisfy the conditions of decomposition scheme (2).

The corresponding response system can then be computed from Eq. (4) and the result is as follows:

$$\begin{aligned}\dot{y}_1 \;=\; & -6y_1 + (\sigma^2 - 6\sigma + \sigma r)x_1 \\ & + (-\sigma^2 + 5\sigma)x_2 - \sigma x_1 x_3, \\ \dot{y}_2 \;=\; & -3y_2 + (-\sigma r + 2r)x_1 + (\sigma r - 2)x_2 \\ & + (\sigma - 2 + b)x_1 x_3 - \sigma x_2 x_3 - x_1^2 x_2, \\ \dot{y}_3 \;=\; & -y_3 + (b^2 - b)x_3 + r x_1^2 + \sigma x_2^2 \\ & - (\sigma + b)x_1 x_2 - x_1^2 x_3.\end{aligned} \tag{11}$$

The differential equations are numerically solved by the Runge–Kutta method. The time step is taken to be 0.01 and 10^4 data points are generated for each x_k and y_l (for all the simulations performed in this work, the Runge–Kutta method is used for integrating the differential equations numerically and the time step is always chosen as 0.01). Since the eigenvalues of $\boldsymbol{A}$ are –6, –3, and –1, the error vector $\boldsymbol{\Delta}(t)$ converges to the zero vector exponentially fast[33] and the state

space of the error system is shown in Fig. 1. In this figure, Δ_1, Δ_2, and Δ_3 are the three elements of the vector $\boldsymbol{\Delta}(t)$. This figure shows that the coincidence between $\dot{x}_k$ and y_k is achieved after some transient time. This can also be verified by the plot of y_k versus $\dot{x}_k$. Figure 2, which is plotted with the 300th data point to the last one (the data points before the 300th data point are discarded to remove transients and hereinafter, unless otherwise specifically mentioned, the figures of y_k versus $\dot{x}_k$ and the ones of state spaces of the driver and the response system are plotted in the same way as that in Fig. 2), shows the plot of y_1 versus $\dot{x}_1$. The plots of y_k versus $\dot{x}_k$ $(k = 2, 3)$ are similar to the plot in Fig. 2, so they are omitted here.

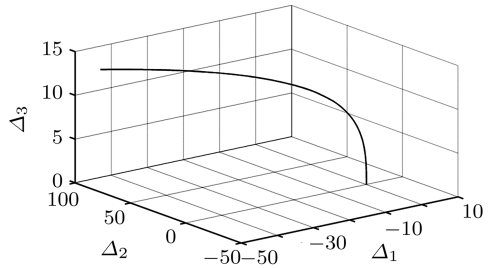


Fig. 1. State space of the error system when $\boldsymbol{A}$ is chosen as that in Eq. (10). All three elements of $\boldsymbol{\Delta}(t)$ converge to zero exponentially fast and this indicates that the state of response system (11) asymptotically approaches the tangent vector of the trajectory of driver (9).

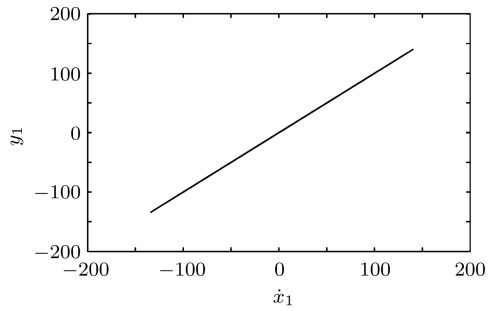


Fig. 2. Plot of y_1 vs. $\dot{x}_1$. The fact that it is located almost on the diagonal verifies the coincidence between $\dot{x}_1$ and y_1.

It is interesting to examine the state space of response system (11), and Fig. 3 shows this from various angles of view. It is obvious that there exists a strange-attractor-like structure in this state space. But it is different from the strange attractor of the Lorenz system with the above parameters. This can be verified by comparing Fig. 3 with Fig. 4, which shows the state space of driver (9). The existence of the strange-attractor-like structure in the state space of response system (11) is related to another interpretation of TR. To specify this, we take the case where the drive system is autonomous as an example. The invariant manifold of systems (3) and (4) is $\boldsymbol{y}(t) = \dot{\boldsymbol{x}}(t)$. Combining it with Eq. (1) yields $\boldsymbol{y}(t) = \boldsymbol{G}(\boldsymbol{x}(t))$, which implies that the state $\boldsymbol{y}(t)$ of response system (4) asymptotically approaches the image of the state $\boldsymbol{x}(t)$ of driver (3) under the nonlinear transformation $\boldsymbol{G}$. This indicates that a special kind of GS[3] occurs between systems (3) and (4), for which the specificity lies in the fact that the functional relationship between $\boldsymbol{x}(t)$ and $\boldsymbol{y}(t)$ is just the function $\boldsymbol{G}$ on the right-hand side of driver (1). In other words, when the coincidence between $\dot{\boldsymbol{x}}(t)$ and $\boldsymbol{y}(t)$ is achieved, we can deem that the coordinate system of the state space of the response system is a nonlinear transformation of the one of the driver. For the Lorenz system with the above parameters, this transformation is a smooth map from $\mathbb{R}^3$ to $\mathbb{R}^3$. But it is not a diffeomorphism because it is not injective (There are three equilibrium points $(6\sqrt{2}, 6\sqrt{2}, 27)$, $(-6\sqrt{2}, -6\sqrt{2}, 27)$, and $(0, 0, 0)$ for the Lorenz system with the above parameters. This indicates that the corresponding transformation is not injective.). Since this coordinate transformation is not a simple translation or rotation, the state space of the driver is distorted by this transformation. This makes the trajectory observed in the state space of the response system a distorted version of the original one in the state space of the driver. Therefore, the strange-attractor-like structure in the state space of response system (11) is the distortion of the strange attractor of driver (9). This new strange-attractor-like structure is similar to the original one since it still has two spirals and there remains a butterfly structure (see the picture in the lower left corner of Fig. 3). However, due to the distortion effect of the nonlinear transformation, it is not identical to the original one. To observe the distortion effect of the nonlinear transformation more clearly, we consider the TR when driver (9) produces an attractive periodic orbit. The parameters in Eq. (9) are chosen as $\sigma = 10$, $r = 350$, and $b = 8/3$, for which the Lorenz system has a globally attracting limit cycle.[34] The matrix $\boldsymbol{A} = \mathrm{diag}(-10, -20, -30)$ and the equations of the corresponding response system, which are omitted here, can be obtained from Eq. (4). 3000 data points are generated for each x_k and y_l. The state spaces of the driver and the response system are plotted with the 1000th data point to the 3000th one and the results are shown in Figs. 5 and 6, respectively. By comparing Fig. 5 with Fig. 6, one can clearly observe that the periodic orbit in Fig. 5 is distorted by the nonlinear transformation.

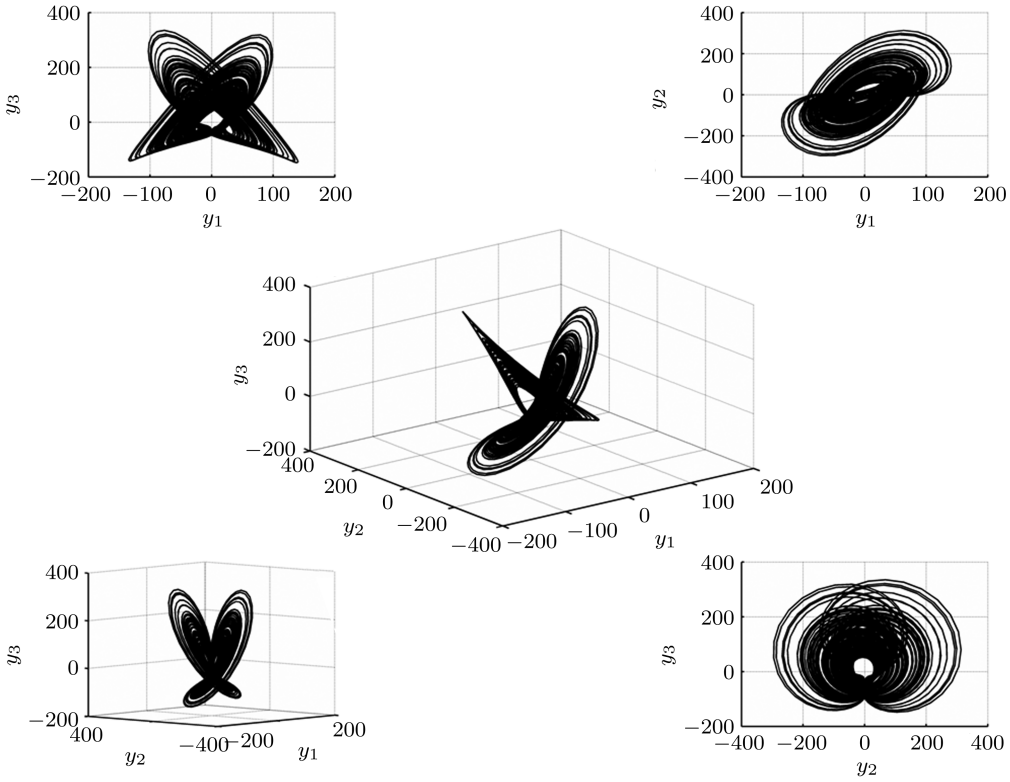


Fig. 3. State space of response system (11). A strange-attractor-like structure exists in it.

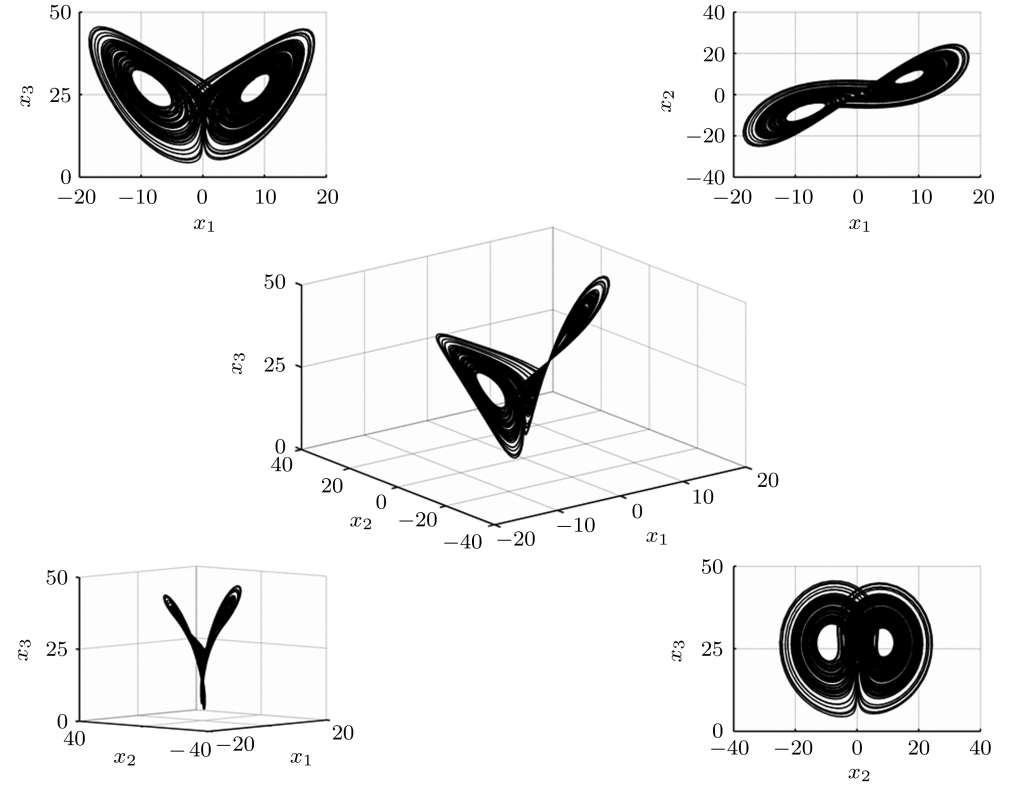


Fig. 4. State space of drive system (9) with the parameters $\sigma = 10$, $r = 28$, and $b = 8/3$. The strange attractor of the Lorenz system is shown from various angles of view.

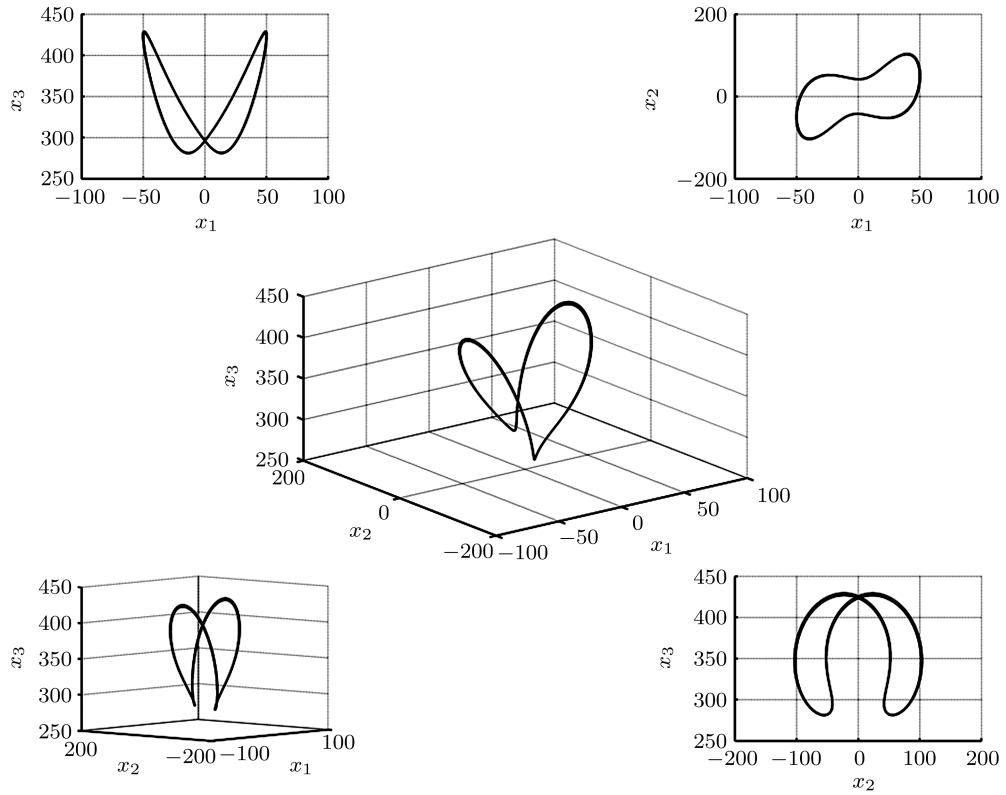


Fig. 5. State space of drive system (9) with the parameters $\sigma = 10$, $r = 350$, and $b = 8/3$. For these parameters, the Lorenz system has a stable periodic trajectory.

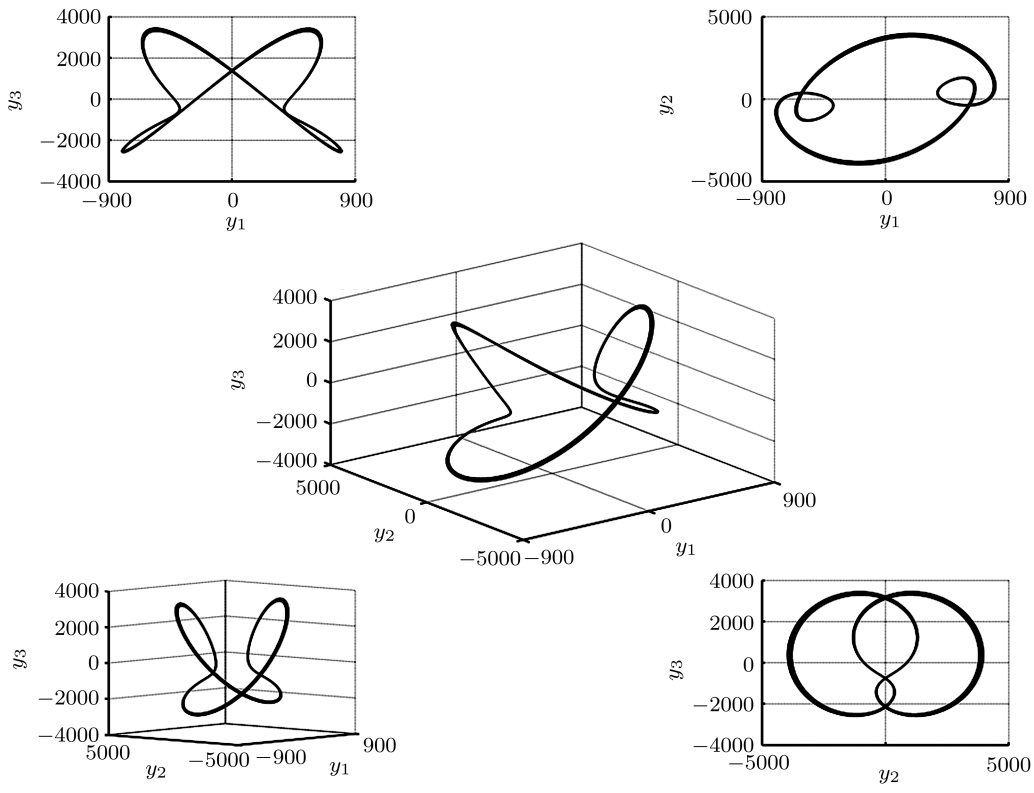


Fig. 6. State space of the response system corresponding to driver (9) with the parameters $\sigma = 10$, $r = 350$, and $b = 8/3$. The periodic trajectory in it is a distortion of the one in Fig. 5.

Now consider another decomposition of the terms on the right-hand side of Eq. (9) with the parameters $\sigma = 10$, $r = 28$, and $b = 8/3$. The matrix A is chosen as

$$\boldsymbol{A} = \begin{bmatrix} -2 & 20 & 0 \\ -20 & -2 & 0 \\ 0 & 0 & -1 \end{bmatrix}, \tag{12}$$

whose eigenvalues are $\lambda_1 = -2 + 20\mathrm{i}$, $\lambda_2 = -2 - 20\mathrm{i}$, and $\lambda_3 = -1$, where i is the imaginary unit. The corresponding response system can be obtained from Eq. (4). All other simulation conditions and parameters are the same as those in Figs. 3 and 4. According to the theory of system of linear first-order ordinary differential equations, the error vector $\boldsymbol{\Delta}(t)$ converges to the zero vector spirally,[33] which is shown in Fig. 7.

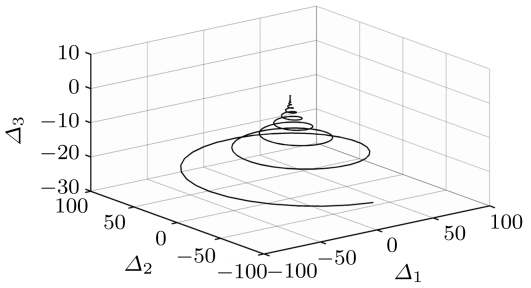


Fig. 7. State space of the error system when $\boldsymbol{A}$ is chosen as that in Eq. (12). The error vector $\boldsymbol{\Delta}(t)$ converges to the zero vector spirally and the coincidence between $\dot{x}_k$ and y_k is achieved asymptotically.

The above simulations demonstrate that the TR is achievable for autonomous drive system (3) and corresponding response system (4). Further, we can control the convergence of the error vector $\boldsymbol{\Delta}(t)$ by adjusting the matrix $\boldsymbol{A}$.

Now we consider the case where the driver is nonautonomous. The driver is chosen as the forced Duffing oscillator, given as

$$\begin{aligned} \dot{x}_1 &= x_2, \\ \dot{x}_2 &= x_1 - x_1^3 - \delta x_2 + p\cos(\omega t), \end{aligned} \tag{13}$$

where $\delta = 0.25$, $p = 0.4$, and $\omega = 1$. This system has the form of Eq. (5) and for this parameter setting, the system has a chaotic attractor.[35] The matrix $\boldsymbol{A}$ is chosen as

$$\boldsymbol{A} = \begin{bmatrix} -3 & 15 \\ -15 & -3 \end{bmatrix}. \tag{14}$$

The corresponding $\boldsymbol{F}(t, \boldsymbol{x}(t))$ can be obtained from Eq. (6). Then according to Eq. (8), the response system can be obtained. 6×10^4 data points are generated for each x_k and y_l. Figures 8 and 9 show the state space of the error system and the plot of y_1 versus $\dot{x}_1$, respectively. These two figures demonstrate that y_k approaches $\dot{x}_k$ asymptotically. To observe the distortion effect of the nonlinear transformation, the state spaces of the response system and the driver are plotted in Figs. 10 and 11, respectively. There is a strange-attractor-like structure in the state space of the response system and according to the above analysis, it is the distortion of the strange attractor in Fig. 11.

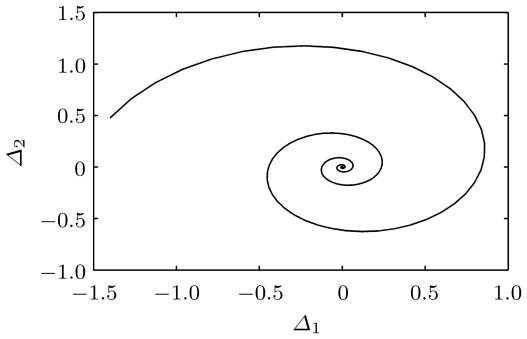


Fig. 8. State space of the error system of driver (13) and the corresponding response system. As the error vector $\boldsymbol{\Delta}(t)$ approaches the zero vector, $\boldsymbol{y}(t)$ approaches $\dot{\boldsymbol{x}}(t)$ asymptotically.

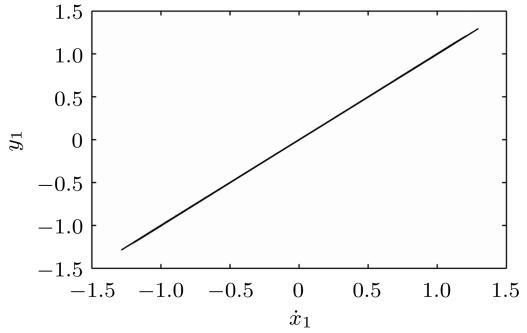


Fig. 9. Plot of y_1 vs. $\dot{x}_1$, which verifies that y_1 converges to $\dot{x}_1$ after some transient time.

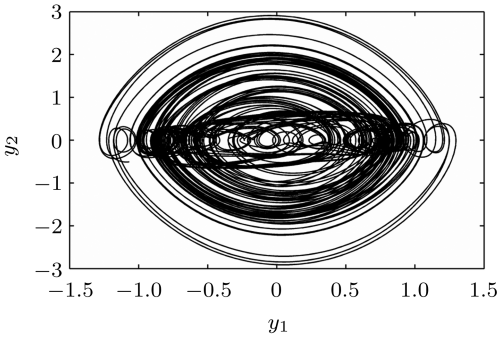


Fig. 10. State space of the response system corresponding to driver (13). The strange-attractor-like structure in this figure is a distorted version of the strange attractor of the forced Duffing oscillator.

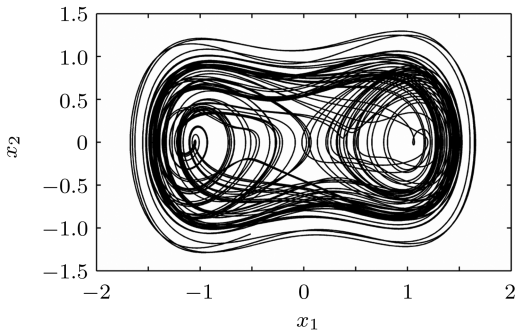


Fig. 11. State space of drive system (13). For the parameters given above, there exists a strange attractor in this state space.

This simulation has demonstrated that if the driver is nonautonomous, then the response system can be constructed according to Eq. (8), which ensures that the TR between systems (7) and (8) is achievable.

In this section, we have verified the validity of the TR schemes by applying them to the Lorenz system and the forced Duffing oscillator. Further, we have pointed out that the TR can also be interpreted as a special kind of GS. In this interpretation, the state space of the response system can be viewed as a distorted version of the one of the drive system. We have visualised this distortion effect by comparing the state spaces of various drivers with the ones of the corresponding response systems.

4. Conclusion

The main work of this paper and its significance can be summarised as follows.

Several different types of synchronisations of coupled chaotic systems are proposed and investigated in the existing literature and for the major classes mentioned in the introduction, the state of the response system has some relationship with the one of the driver. However, in physics one may be concerned about the value of a physical quantity as well as its instantaneous rate of change, which is described by the first-order derivative with respect to time. In this paper, we construct the TR schemes of coupled dynamical systems for autonomous and nonautonomous drivers, respectively. These schemes relate the state of the response system to the first-order derivative of the state of the driver, or more precisely, make the former asymptotically equivalent to the latter, which extends the synchronisation phenomena previously discussed in the literature. The validity of the theoretical analysis is verified by numerical simulations of the Lorenz system and the forced Duffing oscillator.

The time evolution of a dynamical system is represented by a curve in its state space. From a geometric viewpoint, the first-order derivative of the state is the tangent vector of the curve, which evolves as the point moves along the curve. Since the TR schemes make the state of the response system asymptotically approach the tangent vector of the trajectory of the driver, we can track the evolution of the tangent vector by observing the state of the response system. The proposed schemes can also be understood as follows. The evolution of the tangent vector is also a dynamic behaviour, which accompanies the evolution of the state of the driver. The response system describes this behaviour in the asymptotic sense. Information about this behaviour can be obtained by studying the evolution of the response system. When the dimension of the state space of the driver is less than or equal to three, we can plot the trajectory of the response system in its own state space to visualise this dynamic behaviour, as we have done in the simulations.

Besides the above interpretation of TR, it can also be interpreted as a special kind of GS. This interpretation shows that after some transient time, the coordinate system of the state space of the response system is a nonlinear transformation of the one of the driver. So the attractor structure of the driver appears in the state space of the response system in a distorted way and this is why the response system can exhibit rich geometrical structures, such as a strange-attractor-like structure, in its state space.

The previous research has shown that the GS is robust to parameter changes and noise and it can be used to construct secure communication systems.[4,27,36] Since the TR is a special kind of GS, the proposed schemes may have potential applications in the field of secure communications.

References

[1] Pecora L M and Carroll T L 1990 *Phys. Rev. Lett.* **64** 821
[2] Lu J and Cao J 2005 *Chaos* **15** 043901
[3] Rulkov N F, Sushchik M M, Tsimring L S and Abarbanel H D I 1995 *Phys. Rev.* E **51** 980
[4] Kocarev L and Parlitz U 1996 *Phys. Rev. Lett.* **76** 1816
[5] Abarbanel H D I, Rulkov N F and Sushchik M M 1996

Phys. Rev. E **53** 4528
[6] Brown R 1998 *Phys. Rev. Lett.* **81** 4835
[7] Rogers E A, Kalra R, Schroll R D, Uchida A, Lathrop D P and Roy R 2004 *Phys. Rev. Lett.* **93** 084101
[8] Li D and Zheng Z G 2008 *Chin. Phys.* B **17** 4009
[9] Rosenblum M G, Pikovsky A S and Kurths J 1996 *Phys. Rev. Lett.* **76** 1804
[10] Parlitz U, Junge L, Lauterborn W and Kocarev L 1996 *Phys. Rev.* E **54** 2115
[11] Pikovsky A S, Rosenblum M G, Osipov G V and Kurths J 1997 *Physica* D **104** 219
[12] Rosenblum M G, Pikovsky A S and Kurths J 1997 *Phys. Rev. Lett.* **78** 4193
[13] Boccaletti S and Valladares D L 2000 *Phys. Rev.* E **62** 7497
[14] Shahverdiev E M, Sivaprakasam S and Shore K A 2002 *Phys. Lett.* A **292** 320
[15] Zhang H G, Ma T D, Fu J and Tong S C 2009 *Chin. Phys.* B **18** 3751
[16] Voss H U 2000 *Phys. Rev.* E **61** 5115
[17] Masoller C 2001 *Phys. Rev. Lett.* **86** 2782
[18] Sivaprakasam S, Shahverdiev E M, Spencer P S and Shore K A 2001 *Phys. Rev. Lett.* **87** 154101
[19] Shahverdiev E M, Sivaprakasam S and Shore K A 2002 *Phys. Rev.* E **66** 017204
[20] Mainieri R and Rehacek J 1999 *Phys. Rev. Lett.* **82** 3042
[21] Xu D 2001 *Phys. Rev.* E **63** 027201
[22] Li G H 2006 *Chaos, Solitons and Fractals* **29** 490
[23] Parlitz U, Chua L O, Kocarev L, Halle K S and Shang A 1992 *Int. J. Bifurc. Chaos* **2** 973
[24] Kocarev L and Parlitz U 1995 *Phys. Rev. Lett.* **74** 5028
[25] Parlitz U, Kocarev L, Stojanovski T and Preckel H 1996 *Phys. Rev.* E **53** 4351
[26] Liao T L and Tsai S H 2000 *Chaos, Solitons and Fractals* **11** 1387
[27] Terry J R and VanWiggeren G D 2001 *Chaos, Solitons and Fractals* **12** 145
[28] Feki M 2003 *Chaos, Solitons and Fractals* **18** 141
[29] Brown R and Kocarev L 2000 *Chaos* **10** 344
[30] Yu H J and Liu Y Z 2003 *Phys. Lett.* A **314** 292
[31] Chantov D P 2008 *Phys. Lett.* A **372** 5783
[32] Lorenz E N 1963 *J. Atm. Sci.* **20** 130
[33] Hirsch M W, Smale S and Devaney R L 2004 *Differential Equations, Dynamical Systems, and An Introduction to Chaos* (Second Edition) (San Diego: Academic Press)
[34] Strogatz S H 1994 *Nonlinear Dynamics and Chaos: With Applications to Physics, Biology, Chemistry, and Engineering* (Massachusetts: Perseus Books, Reading)
[35] Robinson R C 2004 *An Introduction to Dynamical Systems: Continuous and Discrete* (New Jersey: Pearson Prentice Hall)
[36] Brucoli M, Cafagna D, Carnimeo L and Grassi G 1999 *Int. J. Bifurc. Chaos* **9** 2027